



Photonic molecules for improving the optical response of macroporous silicon photonic crystals for gas sensing purposes

D. CARDADOR,* D. SEGURA, AND A. RODRÍGUEZ

Micro i Nanotecnologies, Departament d'Enginyeria Electrònica, Universitat Politècnica de Catalunya, C/Jordi Girona, 31, 08031, Barcelona, Spain

*david.cardador@upc.edu

Abstract: In this paper, we report the benefits of working with photonic molecules in macroporous silicon photonic crystals. In particular, we theoretically and experimentally demonstrate that the optical properties of a resonant peak produced by a single photonic atom of 2.6 μm wide can be sequentially improved if a second and a third cavity of the same length are introduced in the structure. As a consequence of that, the base of the peak is reduced from 500 nm to 100 nm, while its amplitude remains constant, increasing its Q-factor from its initial value of 25 up to 175. In addition, the bandgap is enlarged almost twice and the noise within it is mostly eliminated. In this study we also provide a way of reducing the amplitude of one or two peaks, depending whether we are in the two- or three-cavity case, by modifying the length of the involved photonic molecules so that the remainder can be used to measure gas by spectroscopic methods.

© 2018 Optical Society of America under the terms of the [OSA Open Access Publishing Agreement](#)

OCIS codes: (160.5298) Photonic crystals; (140.3945) Microcavities; (050.6875) Three-dimensional fabrication.

References and links

1. M. Bayer, T. Gutbrod, J. P. Reithmaier, A. Forchel, T. L. Reinecke, P. A. Knipp, A. A. Dremin, and V. D. Kulakovskii, "Optical Modes in Photonic Molecules," *Phys. Rev. Lett.* **81**(12), 2582–2585 (1998).
2. Y. P. Rakovich and J. F. Donegan, "Photonic atoms and molecules," *Laser Photonics Rev.* **4**(2), 179–191 (2010).
3. K. J. Vahala, "Optical microcavities," *Nature* **424**(6950), 839–846 (2003).
4. F. Vollmer and L. Yang, "Label-free detection with high-Q microcavities: a review of biosensing mechanisms for integrated devices," *Nanophotonics* **1**(3–4), 267–291 (2012).
5. V. M. N. Passaro, B. Troia, M. La Notte, and F. De Leonardis, "Photonic resonant microcavities for chemical and biochemical sensing," *RSC Advances* **3**(1), 25–44 (2013).
6. S. Chakravarty, X. Chen, N. Tang, W.-C. Lai, Y. Zou, H. Yan, and R. T. Chen, "Review of design principles of 2D photonic crystal microcavity biosensors in silicon and their applications," *Front. Optoelectron.* **9**(2), 206–224 (2016).
7. H. Rong, S. Xu, Y.-H. Kuo, V. Sih, O. Cohen, O. Raday, and M. Paniccia, "Low-threshold continuous-wave Raman silicon laser," *Nat. Photonics* **1**(4), 232–237 (2007).
8. Y. Takahashi, Y. Inui, M. Chihara, T. Asano, R. Terawaki, and S. Noda, "A micrometre-scale Raman silicon laser with a microwatt threshold," *Nature* **498**(7455), 470–474 (2013).
9. X.-F. Jiang, C.-L. Zou, L. Wang, Q. Gong, and Y.-F. Xiao, "Whispering-gallery microcavities with unidirectional laser emission," *Laser Photonics Rev.* **10**(1), 40–61 (2016).
10. A. Melloni, F. Morichetti, and M. Martinelli, "Linear and nonlinear pulse propagation in coupled resonator slow-wave optical structures," *Opt. Quantum Electron.* **35**(4/5), 365–379 (2003).
11. F. Xia, L. Sekaric, and Y. Vlasov, "Ultra-compact optical buffers on a silicon chip," *Nat. Photonics* **1**(1), 65–71 (2007).
12. N. Caselli, F. Riboli, F. La China, A. Gerardino, L. Li, E. H. Linfield, F. Pagliano, A. Fiore, F. Intonti, and M. Gurioli, "Tailoring the Photon Hopping by Nearest-Neighbor and Next-Nearest-Neighbor Interaction in Photonic Arrays," *ACS Photonics* **2**(5), 565–571 (2015).
13. Y. Zhao, C. Qian, K. Qiu, Y. Gao, and X. Xu, "Ultrafast optical switching using photonic molecules in photonic crystal waveguides," *Opt. Express* **23**(7), 9211–9220 (2015).
14. X. Zhang, S. Chakravarty, C.-J. Chung, Z. Pan, H. Yan, and R. T. Chen, "Ultra-compact and wide-spectrum-range thermo-optic switch based on silicon coupled photonic crystal microcavities," *Appl. Phys. Lett.* **107**(22), 221104 (2015).
15. S. Bose, D. G. Angelakis, and D. Burgarth, "Transfer of a Polaritonic Qubit through a Coupled Cavity Array," *J. Mod. Opt.* **54**(13–15), 2307–2314 (2007).

16. J. Cho, D. G. Angelakis, and S. Bose, "Heralded generation of entanglement with coupled cavities," *Phys. Rev. A* **78**(2), 022323 (2008).
17. H. Du, X. Zhang, G. Chen, J. Deng, F. S. Chau, and G. Zhou, "Precise control of coupling strength in photonic molecules over a wide range using nanoelectromechanical systems," *Sci. Rep.* **6**(1), 24766 (2016).
18. T. Siegle, S. Schierle, S. Kraemmer, B. Richter, S. F. Wondimu, P. Schuch, C. Koos, and H. Kalt, "Photonic molecules with a tunable inter-cavity gap," *Light Sci. Appl.* **6**(3), e16224 (2016).
19. S. V. Boriskina, "Theoretical prediction of a dramatic Q-factor enhancement and degeneracy removal of whispering gallery modes in symmetrical photonic molecules," *Opt. Lett.* **31**(3), 338 (2006).
20. M. Benyoucef, J.-B. Shim, J. Wiersig, and O. G. Schmidt, "Quality-factor enhancement of supermodes in coupled microdisks," *Opt. Lett.* **36**(8), 1317 (2011).
21. H. Xu, P. Wu, C. Zhu, A. Elbaz, and Z. Z. Gu, "Photonic crystal for gas sensing," *J. Mater. Chem. C Mater. Opt. Electron. Devices* **1**(38), 6087–6098 (2013).
22. D. Cardador, D. Vega, D. Segura, T. Trifonov, and A. Rodríguez, "Enhanced geometries of macroporous silicon photonic crystals for optical gas sensing applications," *Photon. Nanostruct.–Fundam. Appl.* **25**, 46–51 (2017).
23. J. Hodgkinson and R. P. Tatam, "Optical gas sensing: a review," *Meas. Sci. Technol.* **24**(1), 012004 (2013).
24. S. Lan, S. Nishikawa, Y. Sugimoto, N. Ikeda, K. Asakawa, and H. Ishikawa, "Analysis of defect coupling in one- and two-dimensional photonic crystals," *Phys. Rev. B* **65**(16), 165208 (2002).
25. D. Cardador, D. Segura, D. Vega, and A. Rodríguez, "Coupling defects in macroporous silicon photonic crystals," in *2017 Spanish Conference on Electron Devices (CDE) (IEEE, 2017)*, pp. 1–3.
26. B. J. Frey, D. B. Leviton, and T. J. Madison, "Temperature-dependent refractive index of silicon and germanium," *Proc. SPIE* **6273**, 62732J (2006).
27. D. Vega, D. Cardador, M. Garín, T. Trifonov, and A. Rodríguez, "The Effect of Absorption Losses on the Optical Behaviour of Macroporous Silicon Photonic Crystal Selective Filters," *J. Lightwave Technol.* **34**(4), 1281–1287 (2016).
28. A. Goldman, L. R. Brown, W. G. Schoenfeld, M. N. Spencer, C. Chackerian, Jr., L. P. Giver, H. Dothe, C. P. Rinsland, L. H. Coudert, V. Dana, and J.-Y. Mandin, "Nitric oxide line parameters: review of 1996 hitran update and new results," *J. Quant. Spectrosc. Radiat. Transf.* **60**(5), 825–838 (1998).
29. J. M. Parnis and K. B. Oldham, "Beyond the Beer–Lambert law: The dependence of absorbance on time in photochemistry," *J. Photochem. Photobiol. Chem.* **267**, 6–10 (2013).
30. M. Bayindir, B. Temelkuran, and E. Ozbay, "Tight-Binding Description of the Coupled Defect Modes in Three-Dimensional Photonic Crystals," *Phys. Rev. Lett.* **84**(10), 2140–2143 (2000).
31. M. Bayindir, C. Kural, and E. Ozbay, "Coupled optical microcavities in one-dimensional photonic bandgap structures," *J. Opt. A, Pure Appl. Opt.* **3**(6), S184–S189 (2001).
32. T. D. Happ, M. Kamp, A. Forchel, A. V. Bazhenov, I. I. Tartakovskii, A. Gorbunov, and V. D. Kulakovskii, "Coupling of point-defect microcavities in two-dimensional photonic-crystal slabs," *J. Opt. Soc. Am. B* **20**(2), 373–378 (2003).
33. L. Xu-Sheng, C. Xiong-Wen, and L. Sheng, "Investigation and Modification of Coupling of Photonic Crystal Defects," *Chin. Phys. Lett.* **22**(7), 1698–1701 (2005).
34. P. Törmä and W. L. Barnes, "Strong coupling between surface plasmon polaritons and emitters: a review," *Rep. Prog. Phys.* **78**(1), 013901 (2015).
35. S. R.-K. Rodríguez, "Classical and quantum distinctions between weak and strong coupling," *Eur. J. Phys.* **37**(2), 025802 (2016).
36. M. Maksimovic, M. Hammer, and E. W. C. van Groesen, "Coupled optical defect microcavities in 1D photonic crystals and quasi-normal modes," *Proc. SPIE* **6896**, 689603 (2008).
37. A. Majumdar, A. Rundquist, M. Bajcsy, and J. Vučković, "Cavity quantum electrodynamics with a single quantum dot coupled to a photonic molecule," *Phys. Rev. B* **86**(4), 045315 (2012).
38. D. Cardador, D. Vega, D. Segura, and A. Rodríguez, "Study of resonant modes in a 700nm pitch macroporous silicon photonic crystal," *Infrared Phys. Technol.* **80**, 6–10 (2017).
39. S. Matthias, R. Hillebrand, F. Müller, and U. Gösele, "Macroporous silicon: Homogeneity investigations and fabrication tolerances of a simple cubic three-dimensional photonic crystal," *J. Appl. Phys.* **99**(11), 113102 (2006).
40. D. Segura, D. Vega, D. Cardador, and A. Rodríguez, "Effect of fabrication tolerances in macroporous silicon photonic crystals," *Biol. Chem.* **186**, 580–588 (2017).
41. J. Hodgkinson, R. Smith, W. O. Ho, J. R. Saffell, and R. P. Tatam, "Non-dispersive infra-red (NDIR) measurement of carbon dioxide at 4.2 μ m in a compact and optically efficient sensor," *Sens. Actuat. B Chem.* **264**, 172–179 (2013).
42. D. M. Beggs, *Computational Studies of One and Two-Dimensional Photonic Microstructures* (Durham University, 2006).
43. V. S. Boriskina, *Photonic Molecules and Spectral Engineering in Photonic microresonator research and applications* (Springer, 2010), chap. 16.
44. K. Staliunas and V. J. Sánchez-Morcillo, "Spatial filtering of light by chirped photonic crystals," *Phys. Rev. A* **79**(5), 053807 (2009).

1. Introduction

Photonic Molecules (PMs), understood as two or more coupled micro or nanocavities, also called photonic atoms, have been extensively studied during the recent years thanks to their unique optical characteristics [1,2]. As largely reported, a single cavity inserted in a photonic structure has the property of strong photon confinement [3], what can be used in several applications, such as biosensing [4–6], lasing [7–9] and a large etcetera. If a new cavity or a set of them is added to the structure, the optical response cannot only be enhanced but also new functionalities of the system can be obtained. Photon hopping, which consists in the energy transference between adjacent cavities, is one of the most relevant properties of PMs that find its application in coupled-resonator optical waveguides [10–12], optical switching [13,14] or quantum information processing [15,16], among others. Furthermore, it has been shown that this energy transfer can be tuned depending on the inter-cavities conformation and on the morphology of the cavities themselves [17,18], leading to enhanced bandwidths and boosted Q-factors [19,20]. In this work we take advantage of the benefits of using photonic molecules for improving the optical response of macroporous silicon Photonic Crystals (PCs). In concrete, we show how by coupling several photonic atoms and by reshaping them, it is possible to obtain greater Q-factors, larger bandgaps and better filtering along the bandgap, three figures of merit for spectroscopic gas sensing.

Spectroscopic gas detection can be made using photonic crystals by adding a defect in the structure. If it is correctly designed, a transmission peak will arise inside the forbidden band, acting as a narrow band pass filter [21,22]. If this peak is centered in the absorption band of the analyzed gas, its concentration can be determined by means of Non Dispersive Infra-Red methods (NDIR) that basically consist in calculating the area under the intensity line of the peak [23]. For a proper detection, the receiver must work within the bandgap, enveloping the peak. In that sense, the greater the bandgap, the less selective the detector has to be and, thus, the cheaper the final device would be. Besides, it is also necessary to eliminate all the noise in the bandgap since it reduces the performance of the sensor. Therefore, another requirement of the photonic crystals is that the transmission along the bandgap, except for the peak area, has to be as low as possible. Finally, and linked to the previous requirement, the peak transmission should be the maximum possible in order to obtain the greatest sensitivity when determining the amount of gas concentration.

As pointed above, we incorporate new cavities in our macroporous silicon photonic crystals in order to enhance the optical response of the single-cavity case and make these structures suitable for spectroscopic gas sensing. In particular, the study starts showing the poor optical response when only one defect is used. Next, we analyze the transmitted response of our structure when a new cavity is inserted in it. As predicted in literature for one- and two-dimensional PCs, and reported in preliminary studies in 3D, a new peak raises in the bandgap, preserving its transmission and increasing the Q-factor of both peaks [24,25]. Not only this, the bandgap is enlarged and the transmission baseline—also called *offset* along this study—is reduced because more periods have been added in order to place the new cavity. Then, we corroborate this experimentally, showing narrower peaks and better figures for the bandgap. In order to filter one of the two peaks, we shorten the deeper cavity for varying the phase between the two resonant frequencies and we use a chirp modulation, consisting of a linear decreasing of the length of the periods involved in the PC, to optimize the filtering of the resonant states given in the second cavity. This procedure can be extrapolated to the case of three defects, showing a substantial improving of the optical figures respect to the previous cases.

2. Experimental and simulations

Simulations

Simulations have been done using the Optiwave's OptiFDTD software. This tool uses the Finite-Difference Time-Domain method (FDTD) to simulate the propagation of electromagnetic waves along complex structures. Taking advantage of the symmetries of the structures, periodic boundary conditions can be defined to reduce the simulation complexity and time. In our case, the studied photonic crystal can be reduced to a single pore aligned to the Z axis—see Fig. 1, upper image—with periodic boundary conditions on the side walls— XZ and YZ —and multiple perfect absorbing layers before and after the emitter and the receiver, respectively. The front illumination has been done with a Gaussian modulated continuous wave with a linewidth of $\Delta\lambda = 4\mu\text{m}$ and a central wavelength $\lambda_{\text{src}} = 5.2\mu\text{m}$. The transmission spectrum has been obtained by placing a plane detector $5\mu\text{m}$ after the ending of the pore and it has been calculated by integrating the power flux through the detector plane, normalized to the incident wave.

The refractive index of air and silicon, have been respectively set to $n=1.00$ and $n=3.43$ —that corresponds to the average value of silicon in the MIR range at room temperature [26]. Regarding to previous studies, where it was reported that the absorption in low doped silicon has almost no effect on the propagation of light along the PC [27], we did not consider losses in the bulk material. However, as it can be observed in Figs. 2 and 3, simulated results present higher transmissions than the experimental ones. This has its explanation in the fact that the simulations does not consider bulk silicon while in the samples there is a thickness of about $240\mu\text{m}$ continuing the photonic crystal and, hence, they absorb a large part of the transmitted signal. Unfortunately, simulating this rear silicon would lead to unaffordable times of simulations, making unfeasible the direct comparison between experimental and simulated results. However, this drawback can be experimentally solved by removing much of the bulk silicon of the samples—about $150\mu\text{m}$ —as done in the last step of our report.

For the last simulation, air has been replaced by Nitric Oxide (NO), a gas that comprises the wavelength range of the transmitted peak. Following the same procedure as in previous studies [22], the contour of its absorption cross section, obtained through HITRAN database [28], has been approximated by two Lorentzian curves and introduced in OptiFDTD. The amplitude of these curves has been arbitrarily varied to see the evolution of the peak when exposed to different gas concentrations. To relate both, the amplitude of the peak—that takes the 100%, 85%, 72% and 60% of the initial value—and the concentration, we have assumed that the peak is narrow enough to infer the evolution just by studying its central frequency by using Beer-Lambert formula. Therefore, the relationship is given through the absorbance—understood as the logarithm of the ratio between the peak intensity when exposed to some gas concentration and the intensity of the peak when there is no gas in the ambient [29]. A simple calculation revealed that by arbitrary fixing the gas interaction path length to 10 cm —an admissible size for a commercial gas cell—the four studied amplitudes imply concentrations of 0 ppm, 1000 ppm, 2000 ppm and 3000 ppm.

Some considerations about the pore structure

The simulated pores are the result of concatenating multiple thin disks with the appropriated radius in order to emulate the photonic crystals fabricated in our lab that, basically, they consist on a series of modulated areas separated by cavities. As reported in previous studies related to 3D macroporous silicon structures, the number of periods, N , introduced in the modulation areas will affect both the quality factor and the amplitude of the transmission peak [22]. However, despite the fact that for a single cavity case it is reported that eight is the number of periods that maximizes the balance between the transmission and the quality factor of the PC, in this study, where we couple several cavities, we opted to use $N = 5$ for two main

reasons. The first and the most important one is because the coupling between cavities inversely depends on the separation between them, among other features [30–33]. In concrete, if the number of periods between cavities increase, the coupling decreases and therefore, the transmission peaks are closer. In the counterpart, if N decreases, the PC goes towards strong-coupling regime—defined as Törma and Barnes proposed [34,35]—and the peaks become more separated [36,37]. As it will be explained, this separation helps to increase the bandgap and also allows to eliminate undesired transmission peak. The second reason of operating with 5 periods per modulation area is because the number of total periods increase as we add new cavities in the photonic crystal. As a consequence of this, the peak's transmission gets lower because of suffering more interferences in the material's interfaces.

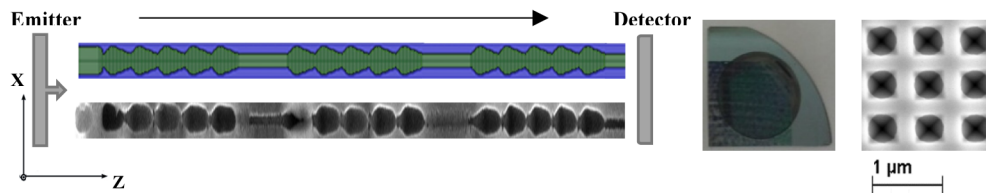


Fig. 1. Left: Schematic representation of the structure and its mode of operation. The source emits light that travels through the photonic crystal. Modulation areas create the bandgap and cavities allow some transmission within it. (Up) and (down), simulated and fabricated profile in the periodical case, respectively. Middle: picture of one of the manufactured samples. All of them have an attached round area of about 1 cm in diameter. Right: top-view of the sample where the array of inverted pyramids of 700 nm pitch is depicted.

Although the basic structure is common to all simulations, we have to distinguish between the two different types of profiles analyzed in this study, the regular and the chirped. In the first one, and regardless of whether we are in the case of two or three cavities, all the periods involved in the different modulated areas have the same length of about 1.2 μm . In the same way, the cavities are designed equally long with a value of 2.6 μm . The second one, the chirped type profile, has a linear decrement in the periodicity and the length of the cavities involved. Several simulations with different values for the involved parameters were done in order to optimize the optical response of the photonic crystal, obtaining that for the two-cavity case, the periods have to decrease from the initial value of 1.4 μm to 1.0 μm . The length of the top cavity has to be maintained in 2.6 μm but the second has to be readjusted to 2.3 μm to achieve a better filtering. In the three-cavity case, the periods vary from 1.5 μm to 0.9 μm and the cavities has been designed with a length of 3.0 μm , 2.6 μm and 2.2 μm , respectively.

Fabrication of macroporous silicon photonic crystals

The fabrication of photonic crystals follows the procedure reported in previous papers [22,38]; a n-type wafer is treated in such a way that, after a lithography and a tetramethylammonium hydroxide (TMAH) attack, its entire surface is marked by square lattice of inverted pyramids equidistantly distributed. These pyramids will act as nucleation centers where the pores will grow in the electrochemical attack. As reported in the mentioned papers, the resulting PCs operate at the mid-infrared range. According to the simulations, several samples were fabricated in order to accurately reproduce the shape of the optimized pores. In the case of the regular modulation, the vertical period is set to 1.2 μm and the length of both defects to 2.6 μm . In the case of the chirped shape with two cavities, the period starts with 1.4 μm and linearly decreases until 1.0 μm . The length of the top cavity has been maintained in 2.6 μm but the deeper one has been lightly shortened to 2.3 μm . In the case of three cavities, the initial period takes the value of 1.5 μm and the last one, 0.9 μm , while the defect's length, from the top to the bottom, is set to 3.0 μm , 2.6 μm and 2.2 μm , respectively.

The total depth of the fabricated PCs ranges approximately between 25 μm and 35 μm , depending on whether we are in the two- or three-cavities case, resulting in an average of 210

μm of bulk silicon after the pores, since the samples have a thickness of $240\ \mu\text{m}$. In order to boost the transmission, part of the rear silicon—about $150\ \mu\text{m}$ —has been etched with a TMAH attack in the final step of this study, leading an improvement from 5% to 27%.

Middle image of Fig. 1 shows the picture of one of the manufactured samples. Scanning Electron Microscope (SEM) images reveal a great uniformity of the pores in the whole area attacked, accordingly to previous studies [39].

Optical characterization

A Bruker Optic's Vertex 70 FT-IR spectrometer has been used to obtain the transmission response of the fabricated photonic crystals. In concrete, the setting parameters for the aperture and the resolution have been $1\ \text{mm}$ and $4\ \text{cm}^{-1}$, respectively. In addition, the light incidence has been aligned perpendicularly to the sample surface ($\Gamma-M$ direction) and several spots in the attacked area were measured to see the optical dispersion due to internal pore inhomogeneity. As a consequence of the pore uniformity reported above, maximum variations of less than 0.1% in both displacement and amplitude were observed in the area, showing a high reproducibility of the PC's optical response. Finally, the detected signal in the receiver has been normalized to the emittance.

3. Results and discussion

The optical response of the photonic crystal with a single-cavity is depicted in Fig. 2. It is clear that the transmitted peak has not good filtering features; it has a very low quality factor ($Q \sim 25$) and the base, $0.5\ \mu\text{m}$ wide, occupies large part of the $0.8\ \mu\text{m}$ that covers the bandgap area—respectively defined as suggested in previous publications [22,40]. This principal characteristic makes the photonic crystal not suitable for conventional spectroscopic gas sensing since the fingerprint of the main gases are comprised in few hundreds of nanometers—i.e. the CO_2 has its spectrum lines within $4.20\ \mu\text{m}$ and $4.35\ \mu\text{m}$. However, they could be used in a broadband filter detection, following a similar procedure as the described in the paper of Hodgkinson et al. [41].

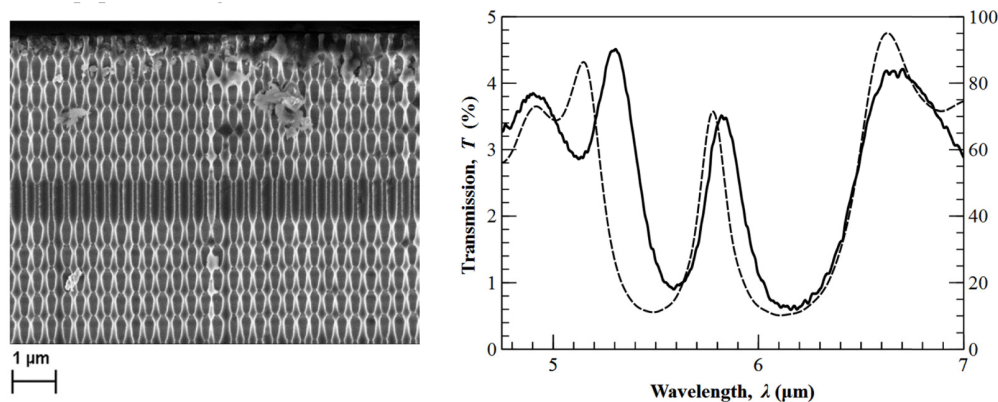


Fig. 2. Left: SEM image of a PC with a single cavity. Right: optical response of the PC for both, experimental (solid line) and simulation (dashed line).

We can also appreciate in Fig. 2 that there is a noticeable transmission percentage along the bandgap area in both, simulation and experimental. We point two main reasons to explain this occurrence. The first one is that the photonic crystal is very short, so the light does not experience enough refractive index changes to fully filter the frequencies inside the bandwidth. The second reason, which concerns only the experimental measures, is that the pores have some degree of inhomogeneity between them, which causes that the filtering in the

bandgap loses some of its efficiency, with respect to the ideal case, among other optical effects [40].

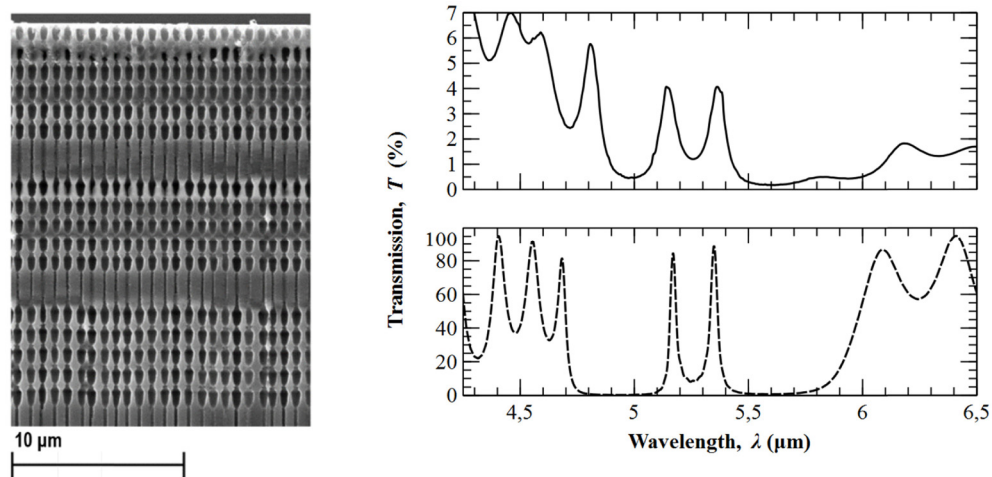


Fig. 3. Left: SEM image of a PC with two cavities with the same value for all periods. Right: in the upper part is depicted the experimental optical response of the PC. The lowest image correspond to the simulations.

According to the literature, if new cavities are introduced, the main peak—that of the case of a single photonic atom—will unfold in as many cavities as have been inserted in the structure. These peaks will have practically the same transmission, but will increase their effective Q-factor due to the narrowing of their base, product of having several coupled resonators [42].

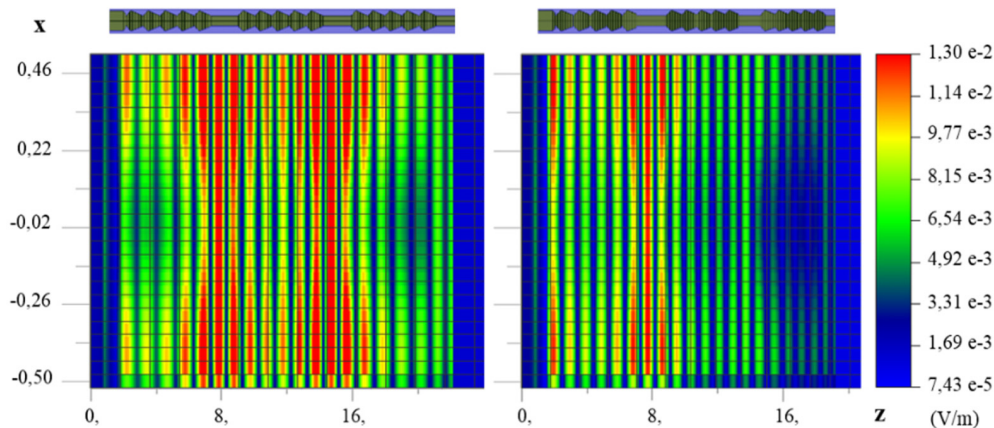


Fig. 4. Section of the pore showing the electrical field (E_z) traveling along the PC. In the left image we can observe that there is the same presence of the field in both cavities (that have higher values than the rest of the PC due to the resonances). In the right image we see that, due to the chirped configuration, the presence of electrical field in the second cavity has been substantially removed. On the top of both images it is depicted the simulated profile.

Taking this into account, we first simulated the structure by adding a new cavity, reporting a significant increment of the Q-factor, a reduction of the offset and a bandgap enlargement. Fabricated samples showed similar results, as can be observed in the Fig. 3. Specifically, we observe that the Q-factor increased by a factor $\times 3$ —going from $Q = 25$ in the case of a single cavity to $Q = 75$ —and the offset was reduced to more than half due to the increase in the

number of periods. In addition, thanks to the introduction of a new peak, the bandgap was widened a 75% more in comparison to the initial case, another of the properties that we wanted to improve.

However, despite the enhancement of the optical features, the transmission characteristics of the PC should be improved to be used as a narrow filter in spectroscopic gas sensing—i.e. the base of the peak is still too wide and the Q-factor and transmission still need to be enhanced. Moreover, the introduction of this new peak is against one of the first premises that we made at the beginning: the elimination of the maximum signal within the operating area of the receiver—except that of the peak that points to the gas. So it would seem that we shot our own foot. Nevertheless, as mentioned in literature, the optical properties of photonic molecules “can be optimally tuned by adjusting the sizes and shapes of individual cavities as well as their positions” [43]. In concrete, the phase between resonant frequencies—and therefore, the transmission of the peaks—can be modified by shortening one of the cavities, showing bonding and antibonding states. In this way, decreasing the second cavity length to $2.3\ \mu\text{m}$, we reduced the transmission of the peak centered in $5.15\ \mu\text{m}$ from 90% to almost 25%. Furthermore, since the chirped modulation has been proved to be an efficient way of filtering light in PC structures [44], we used it to practically filter the whole peak.

As it can be observed in Fig. 4, this new configuration leads to a reduction of the electric field density in the deeper cavity while it is maintained in the top one. As a consequence, the peak with shorter wavelength is substantially reduced while the other does not suffer meaningful modifications—see Fig. 5.

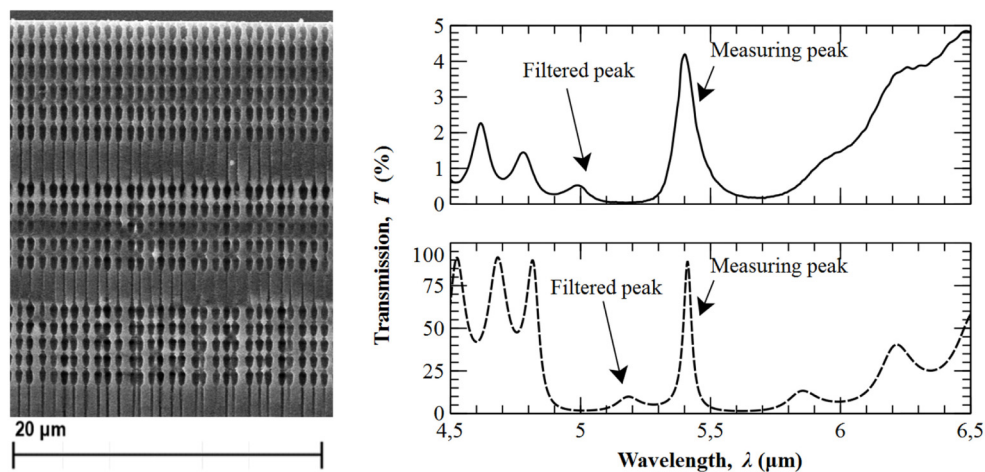


Fig. 5. Left: SEM image of a PC with two cavities in the chirped configuration. Right: optical response of the PC shown in left image for both, experimental (up) and simulation (down).

Using the same arguments, we incorporated a third cavity into the photonic crystal. However, in this case we had greater difficulties when reducing the amplitude of two of the peaks while remaining the other as unaltered as possible. As can be seen in Fig. 6, in the case of same length for the three cavities, the peaks are closer than in the two-cavity case. They can be separated by properly vary the length of the cavities. This leads to a modification in the coupling of the resonant frequencies due to the phase difference what has an impact in the amplitude of the peaks. After several simulations, the optimum spectrum—see image c) of Fig. 6—was reached when the cavities took the values of $3.0\ \mu\text{m}$, $2.6\ \mu\text{m}$ and $2.2\ \mu\text{m}$, going from the top to the bottom. In this figure it can also be seen the appearance of new peaks in the bandgap. These peaks are harmonics of the resonant frequencies that manifest themselves in the forbidden band due to its widening after the incorporation of new cavities. Finally, a chirped modulation—values between $1.5\ \mu\text{m}$ and $0.9\ \mu\text{m}$ —was implemented to further reduce

the amplitude of the *unwanted* peaks. A membrane was made, eliminating a large part of the bulk silicon of the wafer, thereby achieving an increase in the transmission of all the photonic crystal.

The experimental response depicted in the center image of Fig. 7 shows a clear improvement in respect to previous results: the remaining peak increased its experimental Q -factor to approximately $Q = 175$ —2.3 times the one obtained in Fig. 3 and seven times with regard to the single cavity case value, the bandgap width enlarged to $1.5 \mu\text{m}$ and the transmission highly improved from 5% to almost 30%. The transmission base-line, however, did not improve noticeably respect to the two-cavity case because the light is not absorbed in the rear silicon—it was etched—and the photonic crystal does not reflect perfectly the wavelengths inside the bandgap. Nonetheless, the difference between the secondary and the principal peaks is more remarkable and the bandgap width is almost two times the initial case.

The advantages of adding more cavities have a limit: as the system increases in complexity, the peaks are less spaced and new harmonics appear in the bandgap, which ends up having a greater difficulty filtering all the peaks except one. Efforts have been made in this direction and, although it is true that the quality factor of the peaks increases, its filtering has been unsuccessful.

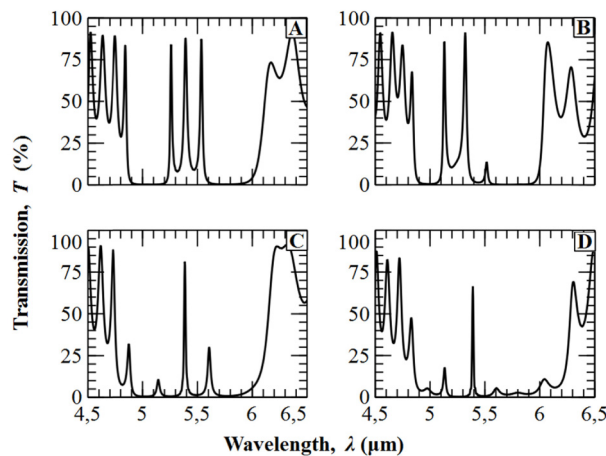


Fig. 6. Optical response of a 3-defect PC (A) when the three cavities have the same length of $2.6 \mu\text{m}$. The variation of the cavities' length has an impact in the amplitude of the involved peaks. In figure (B) we present the coupling of two cavities of $2.2 \mu\text{m}$ and one of $2.6 \mu\text{m}$. In (C) figure, we can observe how the configuration of $3.0 \mu\text{m}$, $2.6 \mu\text{m}$ and $2.2 \mu\text{m}$ arises the central peak and reduce the amplitude of the others. Finally, it is possible to reduce the peaks by applying a chirped modulation (D).

Finally, as a proof of concept, we show in the right image of Fig. 7 the theoretical response of the peak when exposed to different concentrations of nitric oxide at the fixed path length of 10 cm . As it can be seen, its initial amplitude decreases homogeneously for all wavelengths due to the fact that we have almost the same absorption cross section value for all of them. This is in accordance to the assumption made in 'Simulation' section, where we used the approximation of narrow peak to calculate the associated concentrations. In the case of wider peaks, the relationship between the concentration and the amplitude would not be homogenous and integral calculations would be required to accurately determine it [23].

This result can be extrapolated to other gases using the well-known property of scalability in photonic crystals that says that applying a proportionality factor to the geometry, the optical response of the PC is rescaled following the same ratio. Hence, after a proper readjustment of the PC dimensions, the results obtained in this study can be used to sense a number of gases in the MIR region—e.g. CO , CO_2 , NO_2 , NH_3 or CH_4 , among others—that suit the reported absorbance values with lower optical path lengths, as their absorption cross

sections are one or two order of magnitudes bigger than NO's. Therefore, the obtained structures are a promising platform for developing compact and reliable spectroscopic gas sensing.

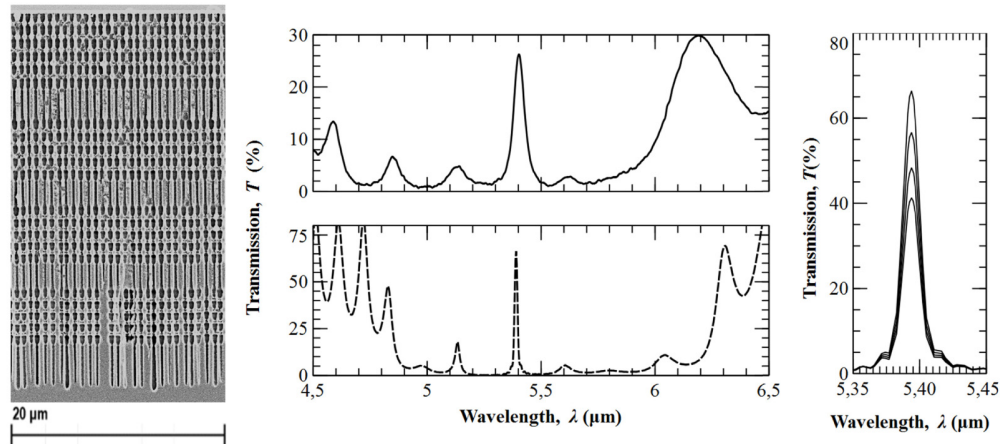


Fig. 7. Left: SEM image of a PC with three cavities in the chirped configuration. Center: comparison between experimental (up) and the simulated results (bottom). Right: peak's transmission decreases as we increase the concentration in steps of 1000 ppm, from 0 ppm to 3000 ppm.

4. Conclusions

To conclude, we have reported a novel way of enhancing the features of macroporous silicon optical filters by means of photonic molecules. In particular it is shown both, experimentally and theoretically, that the introduction of new cavities leads to an enlargement of the bandgap, to a considerable reduction of the noise inside it and to an increasing in the quality factor of the peaks associated to the resonant cavities.

We have also demonstrated that one or two of these peaks can be reduced—and, thus, the bandgap enlarged almost twice with respect to the initial case—by redesigning the photonic crystal structure using a chirped modulation and reducing the cavities' length. Furthermore, we have shown that by performing a membrane, the transmission of the remaining peak reaches almost a 30%, driving it to a quality factor of $Q = 175$. Being both of them the highest values reported for macroporous silicon structures, as far as we know. Finally, a theoretical approach to gas detection has shown that the fabricated PCs are suitable for spectroscopic gas sensing.

Funding

Spanish Ministerio de Economía y Competitividad (MINECO) (TEC-2013-48-147-C6-2).